Multiuser Interference during Synchronization Phase in UWB Impulse Radio

Roman Merz, Cyril Botteron, and Pierre-André Farine
Institute of Microtechnology
University of Neuchâtel, 2000 Neuchâtel
Email: <forename>.<name>@unine.ch

***Abstract*— This paper analyzes the receiver's ability to differentiate between multiple users in ultra-wideband (UWB) impulse radio (IR) during the initial synchronization phase after a cold start, i.e., when the receiver is not yet synchronized with the user of interest. Because of multiple access interference (MAI), the receiver may combine the pulses of other users in a partially coherent way. In this case, the receiver should be able to reject all the interfering users in order to synchronize with the user of interest. For pseudo-random time-hopping (TH) spreading codes, the expected performance of the receiver to differentiate between the user of interest and the interfering users is analyzed and some relations with the code properties are shown. Numerical results for a multipath propagation channel and MAI are provided.**

I. Introduction

Multiple access (MA) and MAI have always been one of the primary concern of wireless communications even since the very first wireless transmissions systems. Indeed, one of the reasons to forbid UWB signals as used in early spark-gap transmitters was the difficulty in discriminating the different transmissions at the receiver [1]. With advances in signal processing, effective methods for code discrimination in UWB communication systems have become applicable. Today, many extensive analyses of performance loss due to MAI have been conducted, in general in terms of lowered signal to noise ratio (SNR) or increased bit error rate (BER). For example, an early contribution (see [2]) discusses the SNR for asynchronous MAI in an additive white Gaussian noise (AWGN) transmission channel, and introduces an approximation using a Gaussian noise to model a large number of interfering users. Same later contributions made by the same working team refine and generalize the results [3]–[7]. These results are confirmed and generalized to BER in [8] and [9]. Extensions to the above results are proposed in [10] using Gaussian quadrature rules. A MAI analysis is also applied to the degradation in distance estimation for positioning systems in [11]. At the University of Oulu, a simulator has been developed to allow the numerical estimation of BER in various environments. In particular, AWGN and multipath propagation channels, narrowband interference (NBI) and MAI can be selected and numerical results for MAI in modified Saleh-Valenzuela channels are presented in [12] and [13]. Deterministic MAI suppression is proposed in [14] and [15] and discussed in [16]. In [17], the concept of deterministic MAI suppression is extended to uplink operation and block-spreading is applied to eliminate the inversion of large matrices. It is shown in [18] that receivers based on deterministic MAI suppression outperform Rake receivers with finite number of fingers, but rely on high sampling rate and training sequences. Finally, [19] analyzes the ability of a receiver to recognize a single transmitting user in a non multipath propagation channel (MAI is thus not considered) without assuming a synchronization with the user of interest.

In this paper, we present a new framework to analyze the receiver's capability to differentiate between users in MAI and multipath channels. As a performance criterion, the gain of the coherent addition of the pulses of the user of interest is compared with the gains of the partially coherent additions of the pulses of the interfering users.

This paper is organized as follows. Section II defines the models to describe the signals in UWB IR, the propagation channel, and the receiver's architecture. In section III, the models are applied to TH spreading. Finally, in section IV a code generator is selected and results from numerical estimations are provided.

II. Models

A. Impulse Radio

An UWB IR communicates by transmitting a succession of very short duration pulses (see Fig. 1). Each symbol is transmitted using a sequence of N_f frames, where each frame contains one pulse. The kth symbol to be transmitted by the mth user is $b_k^{(m)}$. During the transmission of one symbol, a spreading code with amplitude $c_{\mathrm{a},j}^{(m)}$, or time delay $c_{\mathrm{t},j}^{(m)}$ is used, where $0 \leq j < N_\mathrm{f}$ is the index of the pulse during one frame. The spreading codes are used to differentiate between multiple users and to flatten the power spectrum density (PSD). Transmission of the data can be made by amplitude modulation $b_{\mathrm{a},k}^{(m)}$, time delay modulation $b_{\mathrm{t},k}^{(m)}$ or pulse shape modulation $p_{b_k}^{(m)}(t)$. The time shift applied for TH is called the chip duration $T_\mathrm{c}^{(m)}$, the frame duration is $T_\mathrm{f}^{(m)} = N_\mathrm{c} T_\mathrm{c}^{(m)}$, and $T_\mathrm{s}^{(m)} = N_\mathrm{f} T_\mathrm{f}^{(m)}$ is the symbol duration. Denoting the modulation index as $\delta^{(m)}$, the mth transmitter's output signal is

$$s^{(m)}(t) = \sum_{k=-\infty}^{\infty} \sum_{j=0}^{N_\mathrm{f}-1} c_{\mathrm{a},j}^{(m)} b_{\mathrm{a},k}^{(m)} p_{b_k}^{(m)}(t - \tau_{j,k}^{(m)}) \qquad (1)$$

0-7803-9398-8/05/$20.00 ©2005 IEEE

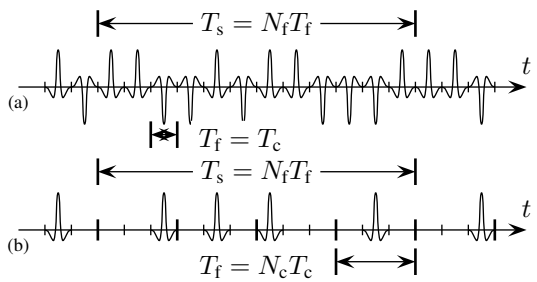

Fig. 1. Typical signals for (a) direct sequence (DS) and (b) TH UWB spreading sequences.

where the time delay $\tau_{j,k}^{(m)}$ is

$$\tau_{j,k}^{(m)} = kT_s^{(m)} - jT_f^{(m)} - c_{t,j}^{(m)}T_c^{(m)} - b_{t,k}^{(m)}\delta^{(m)} - \phi_{j,k}^{(m)}.$$

The additional delay $\phi_{j,k}^{(m)}$ represents an arbitrary time delay between the different users for each transmitted pulse. Using $k = \lfloor l/N_f \rfloor$ with $\lfloor \cdot \rfloor$ the floor operator and $j = \mod(l, N_f)$, it is possible to write the output signal as a single sum over l as

$$s^{(m)}(t) = \sum_{l=-\infty}^{\infty} c_{a,j}^{(m)} b_{a,k}^{(m)} p_{b_k}^{(m)}(t - \tau_{j,k}^{(m)}). \tag{2}$$

The noise-free received signal for the mth user can be written as the convolution between the emitted signal and the impulse response of the mth transmission channel $h^{(m)}(t)$, which is assumed to be static over the period of acquisition, i.e.,

$$r^{(m)}(t) = s^{(m)}(t) * h^{(m)}(t). \tag{3}$$

At the receiver, the signal contains the superposition of the received contributions of each of the M users, some interference $i(t)$ and some white Gaussian noise $\eta(t)$ with two sided power spectral density $\mathcal{N}/2$

$$r(t) = \sum_{m=0}^{M-1} r^{(m)}(t) + i(t) + \eta(t). \tag{4}$$

B. Receiver Architecture

It is well known that a matched filter receiver is optimum in AWGN transmission channels [20]. In a pulse combining receiver where N_f pulses are added coherently, it is possible to first add the individual pulses and then to calculate either the convolution with the impulse response of the matched filter or the correlation with a pulse template afterwards, as long as all intermediate processing is linear. We assume that the receiver acquires a window of finite duration $w_{j,k}(t)$ shorter or equal to the frame duration $T_f^{(0)}$ centered at the moment at which the lth pulse of the user of interest $m = 0$ is assumed to be received, i.e.,

$$w_{j,k}(t) = r(t + \hat{\tau}_{j,k}^{(0)})w(t) \tag{5}$$

where $\hat{x}$ denotes the estimation by the receiver of the respective value x. The fixed window function $w(t)$ limits the duration of the acquired signal, and may be for example a rectangular shape. Note that the window $w(t)$ is assumed large enough such that the lth pulse from the mth user is received completely including multipath arrivals. Because of this assumption, inter-symbol interference (ISI) is not accounted for and the analysis cannot be applied without modification to DS spreading in the configuration where $T_f^{(m)} = T_c^{(m)}$ in multipath propagation channels. However, this assumption is justified in practice for signals using TH spreading sequence with low to medium transmission rates where the frame period is larger than the maximum channel excess delay. We add N_f of these windows to get a summation pulse corresponding to the kth transmitted symbol as

$$w_k(t) = \sum_{j=0}^{N_f-1} w_{j,k}(t). \tag{6}$$

Note that the time window $w_k(t)$ may then be processed further by convolution with the matched filter's impulse response or by correlation with a pulse template generated by the receiver, and a decoder which selects the most probable received symbol. However, as the selected performance criterion is independent of this additional processing in the receiver, we ignore it. The different cases that may arise during the initial synchronization phase are:

(a) The receiver is perfectly synchronized with the user of interest $\hat{\tau}_{j,k}^{(0)} = \tau_{j,k}^{(0)} + \delta$ with a constant time offset δ such that the pulses are still received within the acquisition window. This means that the correct spreading code is used and that the difference in additional delays $\{\hat{\phi}_{j,k}^{(0)} - \phi_{j,k}^{(0)}\}$ is constant for all j, k. This results in a coherent addition of the individual pulses of the user of interest. It is considered as the only correct case to terminate the synchronization phase and serves as a reference.

(b) The difference in additional time delays $\{\hat{\phi}_{j,k}^{(0)} - \phi_{j,k}^{(0)}\}$ is constant for all j, k for the user of interest, and the correct code is applied, but with a phase offset of Δj frames, with $0 < \Delta j < N_f$ and $\hat{c}_{t,j}^{(0)} = c_{t,j\oplus\Delta j}^{(0)}$, where $\oplus$ is the addition modulo N_f. This results in a partially coherent summation of the pulses of the user of interest and may arise during the initial synchronization phase of the receiver.

(c) The difference in additional delays $\{\hat{\phi}_{j,k}^{(0)} - \phi_{j,k}^{(n)}\}$ is constant for all j, k for an interfering user $n \neq 0$, and the code of the user of interest is applied with a phase offset of Δj frames, with $0 \leq \Delta j < N_f$, and $\hat{c}_{t,j}^{(0)} = c_{t,j\oplus\Delta j}^{(0)}$. This results in a partially coherent summation of the pulses of the nth user and may also arise during the initial synchronization phase.

(d) The receiver's additional delay $\hat{\phi}_{j,k}^{(0)}$ is neither related with the additional delay of the user of interest nor with any other user. All additions are incoherent independently of the spreading code.

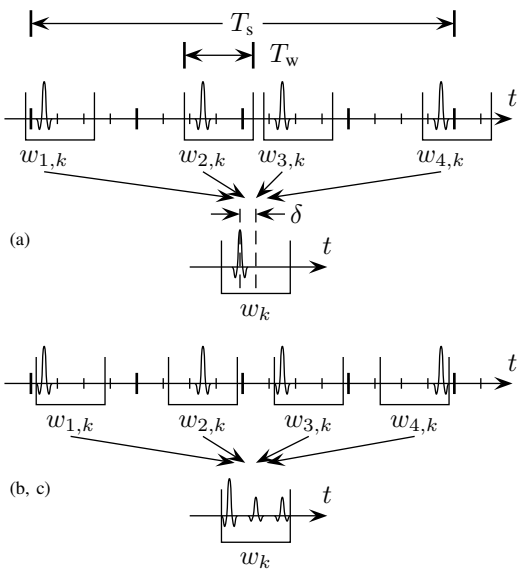

Fig. 2. Coherent (a) and partially coherent (b, c) addition of limited duration windows to obtain a summation pulse for the kth symbol.

A schematic representation of the cases (a) to (c) is shown in Fig. 2. To successfully terminate the synchronization phase, it is important that the receiver can differentiate between the result of the coherent addition (a) and the ones of partially coherent additions (b, c). Clearly, the incoherent addition (d) will have a smaller pulse combining gain compared to (a, b, c), and is not considered further.

C. Performance Measurement

As explained in the introduction, the BER is commonly used to evaluate the performance of a communication system. However, it is not a good benchmark to evaluate what is happening during the synchronization phase. The SNR, on the other hand, can easily be used with unsynchronized systems, but it requires knowledge about the emitted pulse shapes, the propagation channel, and the receiver's architecture. For example, assuming a multipath channel and a Rake receiver, the received energy of the signal will depend on the number and alignment of the individual fingers. To have a performance measurement which is less dependent on the receiver's architecture, and considering that the most simple receiver may operate on the envelope of the received signal, the maximum of the received signal during the acquisition window is taken and defined as $\mathcal{W} = \max_t |w_k(t)|$. The maximum of the received signal in the case of coherent addition (a) is defined as $\mathcal{W}_{(a)}$. $\mathcal{W}_{(b,c)}$ denotes the maximum value of all possible configurations that belong to cases with partially coherent additions (b, c). Finally, we define the distinction coefficient

$$\mathcal{D} = \mathcal{W}_{(a)}/\mathcal{W}_{(b,c)}. \tag{7}$$

It can be related to the probability that the coherent result may be recognized out of partially coherent results. For example, the distinction coefficient $\mathcal{D}$ can be used to estimate the maximum difference in power levels due to near-far effect that can be tolerated by the system, such that the receiver can still acquire the user of interest and not an interfering user.

D. Channel Models

To evaluate the impact of MAI in a non-multipath channel, a perfect channel (PC) with impulse response $h(t) = \delta(t)$, where $\delta(t)$ is the Dirac delta function, is used. To evaluate the performance in a typical indoor multipath channel, the modified Saleh-Valenzuela model CM3, specified in the IEEE 802.15.3a standard [21], is used.

III. Application to Time Hopping

A. Generic Considerations of the Model

For the application to TH spreading sequences, it is assumed that all users use the same pulse shape and the transmission channels are statistically independent. During the transmission of one symbol, the time delay $b_{t,k}^{(m)}\delta^{(m)}$ corresponding to the symbol $b_{t,k}^{(m)}$ is constant and can be neglected as long as the received pulse is still received during the acquisition window. Thus, omitting data modulation, the generated sequence for TH spreading sequence for equal pulse energy is

$$s^{(m)}(t) = \sum_{l=-\infty}^{\infty} p(t - \tau_{j,k}^{(m)}) \tag{8}$$

with $\tau_{j,k}^{(m)} = kT_s^{(m)} - jT_f^{(m)} - c_{t,j}^{(m)}T_c^{(m)} - \phi_{j,k}^{(m)}$ and $j = \mod(l, N_f)$. Assuming a frame-synchronized system and using (3), (4), (5), and (6), the summed signal without interference $i(t)$ becomes

$$\begin{aligned} w_k(t) = &\sum_{j=0}^{N_f-1}\left(\sum_{m=0}^{M-1} q^{(m)}(t - \tau_{j,k}^{(m)} + \hat{\tau}_{j,k}^{(0)})\right) w(t) \\ &+ \sum_{j=0}^{N_f-1} \eta(t + \hat{\tau}_{j,k}^{(0)}) w(t) \end{aligned} \tag{9}$$

where $q^{(m)}(t) = p(t) * h^{(m)}(t)$ denotes the received pulse shape. Note that the above assumption of frame synchronization is not very restrictive, as an unsynchronized case can still be modeled with a frame-synchronized case using the variable $\phi_{j,k}^{(m)}$ such that $\hat{\tau}_{j,k}^{(0)} - \tau_{j,k}^{(m)}$ is uniformly distributed over the common frame duration T_f. The common chip duration is denoted as T_c.

If the time window is rectangular, and recalling that the pulse is received completely during the time window, (9) can be written with respect to the frame synchronized user n as

$$\begin{aligned} w_k(t) = &\sum_{j=0}^{N_f-1} q^{(n)}(t - \tau_{j,k}^{(n)} + \hat{\tau}_{j,k}^{(0)}) \\ &+ \sum_{j=0}^{N_f-1}\sum_{\substack{m=0 \\ m\neq n}}^{M-1} q^{(m)}(t - \tau_{j,k}^{(m)} + \hat{\tau}_{j,k}^{(0)}) \\ &+ \sum_{j=0}^{N_f-1} \eta(t + \hat{\tau}_{j,k}^{(0)}) w(t) \end{aligned} \tag{10}$$

with

$$\hat{\tau}_{j,k}^{(0)} - \tau_{j,k}^{(n)} = \left(c_{\mathrm{t},j}^{(n)} - \hat{c}_{\mathrm{t},j}^{(0)}\right) T_{\mathrm{c}}. \tag{11}$$

The first term in (10) is the principal contribution resulting from coherent (a) or partially coherent additions (b, c). It depends on the properties of the spreading sequence as shown in (11). The second term describes incoherent addition due to MAI. It is zero in the single user case. The third term is white Gaussian noise with variance $N_{\mathrm{f}}\mathcal{N}/2$.

B. Single Access

Only the nth user is assumed to transmit. Thus, without noise, only the first term of (10) remains. For case (a), the maximum is

$$\mathcal{W}_{(\mathrm{a})} = N_{\mathrm{f}} \max_t q^{(0)}(t). \tag{12}$$

Applying the code of the user of interest ($m = 0$), and receiving the signal of user n (cases (b, c)), we get,

$$\mathcal{W}_{(\mathrm{b,c})} = \max_{(\mathrm{b,c})} \max_t \left(\sum_{j=0}^{N_{\mathrm{f}}-1} q^{(n)}(t + (c_{\mathrm{t},j}^{(n)} - c_{\mathrm{t},j\oplus\Delta j}^{(0)})T_{\mathrm{c}}) \right) \tag{13}$$

where $\max_{(\mathrm{b,c})}$ denotes the maximum over all configurations belonging to cases (b, c). We note that the time shift applied to the received pulse shape is completely determined by the spreading codes by $(c_{\mathrm{t},j}^{(n)} - c_{\mathrm{t},j\oplus\Delta j}^{(0)})T_{\mathrm{c}}$. If the shifted pulses do not overlap, i.e. the duration of $q^{(n)}(t)$ is smaller than T_{c}, (13) can be written as

$$\mathcal{W}_{(\mathrm{b,c})} = \mathscr{W}_{(\mathrm{b,c})} \max_t q^{(n)}(t) \tag{14}$$

where $\mathscr{W}_{(\mathrm{b,c})}$ denotes the maximum number of solutions in j to

$$c_{\mathrm{t},j}^{(n)} - c_{\mathrm{t},j\oplus\Delta j}^{(0)} = l \tag{15}$$

for any admissible Δj and l. In PC, $q^{(0)}(t) = q^{(n)}(t)$ and the distinction coefficient $\mathcal{D}$ become independent of the pulse shape. $\mathscr{W}_{(\mathrm{b,c})}$ is referred to as the maximum number of hits between the two delayed TH codes and is studied extensively in [19].

IV. Numerical Results

A. Practical Code

Two illustrative spreading codes are compared. One spreading code is obtained by Matlab's™ random generator. The second spreading code for the mth user $s_j^{(m)}$ is generated by using the following polynomial, describing the taps of a linear feedback shift register (LFSR) implementation [22]

$$\begin{aligned} a_k &= 1 + x^3 + x^{10} \\ b_k &= 1 + x^2 + x^3 + x^6 + x^8 + x^9 + x^{10} \\ d_k^{(m)} &= (a_k + b_{k-m}) \mod 2. \end{aligned} \tag{16}$$

TABLE I

Analytical estimation of $\mathcal{D}$, without MAI, for non-overlapping shifted pulses.

N_{f}	$N_{\mathrm{b}} = 1$ bit		$N_{\mathrm{b}} = 2$ bits		$N_{\mathrm{b}} = 3$ bits	
	RAND	LFSR	RAND	LFSR	RAND	LFSR
2	1.00	1.00	1.00	2.00	2.00	2.00
4	2.00	2.00	2.00	2.00	4.00	2.00
8	1.33	1.33	2.67	2.67	4.00	4.00
16	1.60	1.60	2.67	2.29	4.00	4.00
32	1.45	1.78	2.13	2.67	4.00	4.00
64	1.60	1.68	2.67	2.91	4.27	4.92
128	1.64	1.68	2.67	2.84	4.74	5.57
256	1.73	1.64	2.78	3.12	5.95	5.33

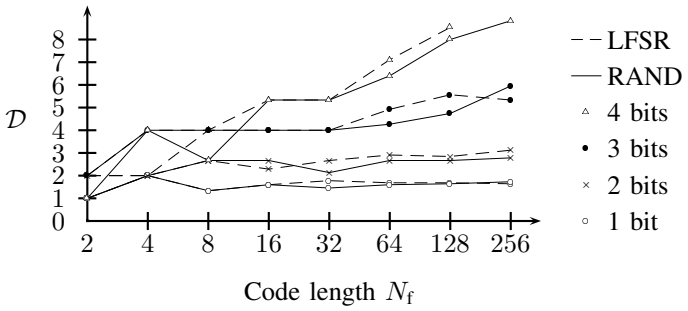

Fig. 3. $\mathcal{D}$ for LFSR and random spreading codes, without MAI, in PC

The spreading code $c_{\mathrm{t},j}^{(m)}$, where each symbol is represented by N_{b} bits, is combined from the first $N_{\mathrm{b}}N_{\mathrm{f}}$ values of the sequence $d_k^{(m)}$, by using

$$c_{\mathrm{t},j}^{(m)} = \sum_{i=0}^{N_{\mathrm{b}}-1} d_{N_{\mathrm{b}}j+i}^{(m)} 2^{N_{\mathrm{b}}-1-i}. \tag{17}$$

B. Description of the Numerical Results

For the numerical results, we assume a 2nd derivative Gaussian pulse defined as

$$p_{\mathrm{G}_2}(t) = \sqrt{\frac{4\varsigma RE}{3t_n}} \left(\frac{t^2}{t_n^2} - 1\right) \exp\left(-\frac{t^2}{2t_n^2}\right) \tag{18}$$

where E is the energy of the pulse assuming an impedance R, t_n is the pulse duration, and $\varsigma = 1/\sqrt{\pi}\,\mathrm{kg\,m^2\,s^{-4}}$ is a normalization coefficient. The pulse's energy is 1 pJ at 50 Ω and the pulse duration is $t_n = 200\,\mathrm{ps}$. The frame duration is 100 ns and the chip duration 1 ns. The received pulse shape $q^{(m)}(t)$ is generated using the transmission channel model and the emitted pulse shape for each user. The received signals of the M users are added, and the distinction coefficient $\mathcal{D}$ estimated.

C. Single Access

The single user access is analytically analyzed using (15) and presented in table I, where the distinction coefficient $\mathcal{D}$ for the random spreading code and the spreading code generated by the LFSR was obtained with varying number of bits to represent the symbols.

The distinction coefficient $\mathcal{D}$ was also evaluated numerically using (12) and (13) (see Fig. 3). As expected, for the user

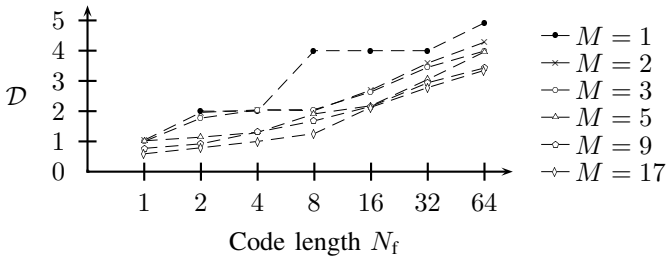

Fig. 4. $\mathcal{D}$ for three bits LFSR code, with MAI, in PC.

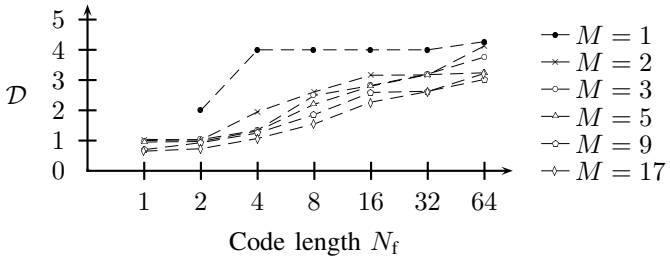

Fig. 5. $\mathcal{D}$ for a three bits random code, with MAI, in PC.

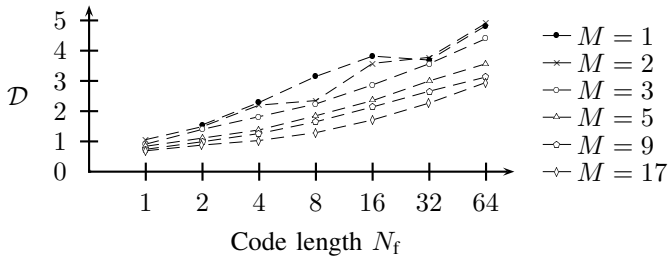

Fig. 6. $\mathcal{D}$ for a three bits LFSR code, with MAI, in CM3 channel model.

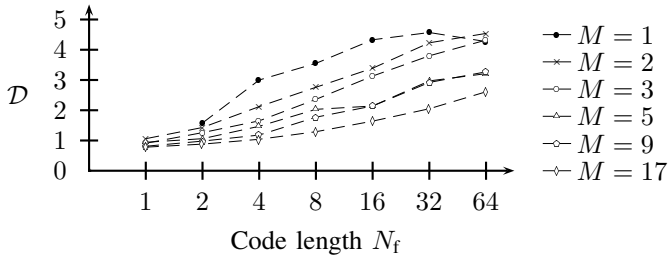

Fig. 7. $\mathcal{D}$ for a three bits random code, with MAI, in CM3 channel model.

$n = 0$ in PC, the numerical results are identical to the analytical ones. Moreover, we note that in order for the distinction coefficient to improve with the length of the code, a sufficient number of bits used to represent the symbols must be used (e.g., no improvement is observed when a single bit per symbol is used). Note that the "meandering" of the distinction coefficient, e.g. the decrease for the 2 bits LFSR spreading code with length 16 compared to a spreading code with length 8, is a consequence of the deterministic selection of the code.

D. Multiple Access Interference

The following numerical results with MAI are obtained using the first two terms of (10). The results of the random and the LFSR spreading code with three bits symbols are represented in Fig. 4 and 5 for PC and Fig. 6 and 7 for CM3 channel model. As expected, the distinction coefficient is degraded for decreasing code length and increasing number of interfering users. The degradation in the distinction coefficient for M users can be attributed to two major contributions. Firstly, for pseudo-random spreading codes, the probability to select a spreading code with bad separation properties increases with additional users. This is the principal cause for the important degradation in Fig. 5 between the results for a single user $M = 1$ and two users $M = 2$. Secondly, the captured pulses from interfering users may alter the maximum of the received signal during the acquisition window due to superposition. In general, the distinction coefficient tend to decrease with increasing number of interfering pulses. As $\mathcal{W}_{(\mathrm{b,c})}$ is the maximum over all configurations belonging to (b, c), it is expected to increase more than $\mathcal{W}_{(\mathrm{a})}$. The effect of interfering pulses can be illustrated with, for example, a spreading code of length 1. In this case, the receiver will not be able to differentiate between the users, independently of the number of bits used to represent the symbols. In fact, the analysis of the code using (15) results in a distinction coefficient of 1. The numerical simulations using (10), as represented in Fig. 4–7, show a distinction coefficient for code length 1 and multiple users smaller than 1. An atypical behavior with an improvement in the distinction coefficient for two users compared to a single user is shown in Fig. 7 for code length 64. We note that this is the outcome of one deterministic arrangement. To isolate the degradation of the distinction coefficient due to incoherently interfering pulses, the difference between the distinction coefficient obtained by a numerical simulation with the first two terms in (10) and the distinction coefficient obtained with the first term only is calculated. The average difference between the distinction coefficient over code length ranging from 1 to 64 for the LFSR and random codes is represented as a function of the number of users M in Fig. 8. We note that the distinction coefficient is more prone to a degradation in a multipath channel than in a PC.

V. Conclusion

In this paper, the receiver's ability to differentiate between the user of interest and the interfering users in TH-UWB during synchronization phase is analyzed for a perfect channel (PC) model and a typical indoor multipath channel. As a benchmark, a distinction coefficient related to the probability of successful termination of the initial synchronization is introduced. This distinction coefficient can also be used, for example, to estimate the maximum difference in power levels due to near-far effect that can be tolerated by the system, such that the receiver can still acquire the user of interest and not an interfering user. It is shown that the distinction coefficient for a single user in the PC model is completely determined by

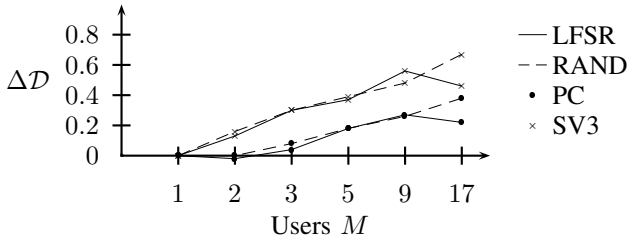

Fig. 8. Degradation of the distinction coefficient due to interfering pulses.

the spreading code properties. Examples of the degradation in MAI due to spreading code properties and interfering pulses are presented based on numerical simulations.

ACKNOWLEDGMENT

The work was supported by the Swiss Center for Electronics and Microtechnology Neuchâtel (http://www.csem.ch) and the Swiss National Fonds (http://www.snf.ch).

REFERENCES

[1] K. Siwiak and D. McKeown, *Ultra-Wideband Radio Technology*. John Wiley & Sons, Ltd., 2004.

[2] R. A. Scholtz, "Multiple access with time-hopping impulse modulation," in *Proc. Military Communications Conference*, vol. 2, Oct. 1993, pp. 447–450, invited Paper.

[3] M. Z. Win and R. A. Scholtz, "Comparisons of analog and digital impulse radio for wireless multiple-access communications," in *Proc. Communications Conf.*, 1997, pp. 91–94.

[4] R. A. Scholtz and M. Z. Win, "Impulse radio," in *Proc. Int. Personal, Indoor and Mobile Radio Communications Symposium*, Helsinki, Sept. 1997, pp. 245–267, invited Paper.

[5] F. Ramírez-Mireles and R. A. Scholtz, "Wireless multiple-access using ss time-hopping and block waveform pulse position modulation part 2: System performance," in *Proceedings ISITA Symposium*, Sept. 1998.

[6] ——, "Multiple-access performance limits with time hopping and pulse position modulation," in *Proc. Military Communications Conference*, vol. 2, Oct. 1998, pp. 529–533.

[7] M. Z. Win and R. A. Scholtz, "Impulse radio: How it works?" *IEEE Commun. Lett.*, vol. 2, no. 2, pp. 36–38, Feb. 1998.

[8] V. S. Somayazulu, "Multiple access performance in uwb systems using time hopping vs. direct sequence spreading," in *Proc. Wireless Communications and Networking Conference*, vol. 2, Mar. 2002, pp. 522–525.

[9] S. Gezici, H. Kobayashi, H. V. Poor, and A. F. Molisch, "Performance evaluation of impulse radio uwb systems with pulse-based polarity randomization in asynchronous multiuser environments," in *Proc. Wireless Communications and Networking Conference*, vol. 2, Mar. 2004, pp. 908–913.

[10] G. Durisi and S. Benedetto, "Performance evaluation of th-ppm uwb systems in the presence of multiuser interference," *IEEE Commun. Lett.*, vol. 7, no. 5, pp. 224–226, May 2003.

[11] C. Mazzucco, U. Spagnolini, and G. Mulas, "A ranging technique for uwb indoor channel based on power delay profile analysis," in *Proc. Vehicular Technology Conference*, 2004.

[12] R. Tesi, M. Hämäläinen, J. Iinatti, I. Oppermann, and V. Hovinen, "On the multi-user interference study for ultra wideband communication system in awgn and modified saleh-valenzuela channel," in *Proc. Int Ultra Wideband Systems Workshop*, May 2004.

[13] R. Tesi, "Ultra wideband system performance in the presence of interference," May 2004, Licentiate Thesis.

[14] C. J. L. Martret and G. B. Giannakis, "All-digital pam impulse radio for multiple-access through frequency-selective multipath," in *Proc. Global Telecommunications Conf.*, vol. 1, 2000, pp. 77–81.

[15] ——, "All-digital impulse radio for mui/isi-resilient multiuser communications over frequency-selective multipath channels," in *Proc. Military Communications Conference*, Oct. 2000, pp. 655–659.

[16] ——, "All-digital impulse radio for wireless cellular system," *IEEE Trans. Commun.*, vol. 50, no. 9, pp. 1440–1450, Sept. 2002.

[17] L. Yang and G. B. Giannakis, "Multistage block-spreading for impulse radio multiple access through isi channels," *IEEE J. Select. Areas in Commun.*, vol. 20, no. 9, Dec. 2002.

[18] ——, "Ultra-wideband communications. an idea whose time has come," *IEEE Signal Processing Mag.*, pp. 26–54, Nov. 2004.

[19] T. Erseghe, "Ultra wide band pulse communications," Ph.D. dissertation, Università Degli Studi Di Padova, 2001.

[20] J. G. Proakis, *Digital Communications*, 4th ed. McGraw-Hill Higher Education, 2001.

[21] J. R. Foerster, M. Pendergrass, and A. F. Molish, "A channel model for ultrawideband indoor communication," *IEEE Trans. Wireless Commun.*, vol. 10, no. 6, pp. 14–21, Dec. 2003.

[22] Arinc Research Corporation, "Navstar gps space segment, navigation user interfaces," July 1991.